The formation each winter of the circumpolar wave in the sea ice around Antarctica

Per Gloersen* and Warren B. White†

* Oceans and Ice Branch, Laboratory for Hydrospheric Sciences, NASA/Goddard Space Flight Center, Greenbelt, Maryland 20771, USA
†Scripps Institution of Oceanography, University of California-San Diego, La Jolla, California 92093-0230, USA

Seeking to improve upon the visualization of the Antarctic Circumpolar Wave (ACW)[1-3], we compare a 16-year sequence of 6-month winter averages of Antarctic sea ice extents and concentrations with those of adjacent sea surface temperatures (SSTs). Here we follow SSTs around the globe along the maximum sea ice edge rather than in a zonal band equatorward of it. The results are similar to the earlier ones, but the ACWs do not propagate with equal amplitude or speed. Additionally in a sequence of 4 polar stereographic plots of these SSTs and sea ice concentrations, we find a remarkable correlation between SST minima and sea ice concentration maxima, even to the extent of matching contours across the ice-sea boundary, in the sector between 90°E and the Palmer Peninsula. Based on these observations, we suggest that the memory of the ACW in the sea ice is carried from one Austral winter to the next by the neighboring SSTs, since the sea ice is nearly absent in the Austral summer.

We use two types of data here to show the Antarctic Circumpolar Wave (ACW) in more detail than was possible before[1-3] when relationships were examined between sea ice and nearby sea surface temperatures (SSTs). The 1982-1996 SSTs are from the dataset prepared by Reynolds[4]. The 1979-1996 sea ice concentrations were prepared at NASA/GSFC and obtained from the National Snow and Ice Data Center[5]. The sea ice concentration data were further processed into extents of sea ice (ESI, in ° latitude, using a 15% ice edge criterion) and average sea ice concentration (ASIC, in percent) in 1°-longitude bins. All of the time sequences were averaged by month, depleted by their respective long-term mean (averages-by-month over their shared record length) to form residuals (or, anomalies) about the mean annual cycle. Subsequently, they were filtered with a band-pass filter[6] with half-power points at 3 and 7 years to reduce, among other things, the seasonal cycle remaining after subtracting its average. Finally all the data sequences were arranged into 6-month averages of June-July-August-September-October-November (JJASON) data, yielding one value for each calendar year, so as to emphasize the connection between SSTs, which are not available near the ice edge in Austral late spring, summer, and early fall[7], and the sea ice.

Time-longitude diagrams (Fig. 1) obtained from the time series of the SSTs, extents of sea ice, and average sea ice concentrations from 1979-1996 are similar but not identical to the ones published earlier[1-3]. Differences in detail result mostly from the residuals being averaged over JJASON to obtain the annual observations of the winter sea ice phenomena. The SST data most clearly show the Antarctic Circumpolar Wave (ACW) described earlier[1-3]. In the ESI and ASIC data, similar waves seem to propagate

at about the same speed as the SST waves but they appear to be confined to the longitudes from about 150°E and eastwards to about 30°E. Hence they appear not to be completely circumpolar during this time period. Indeed, both ASIC and (less clearly) ESI diagrams show propagation in the opposite direction of the ACW during 1980-1985 in the western portion of the diagram. The ESI also displays some retrograde motion in the eastern part of the diagram from 1983-1996. This may have occurred because the ACW follows the Antarctic Circumpolar Current up toward Africa in the Atlantic and Indian Ocean sectors of the Southern Ocean[1-3]. No doubt climate change phenomena other than those associated with the ACW operate in the Southern Ocean as well.

In order to obtain a more detailed view of wave propagation within the sea ice pack than can be obtained from the time/longitude diagram of ASIC, we decomposed the yearly JJASON time series of sea ice concentration (SIC) grid maps into complex empirical orthogonal functions (CEOFs). We accomplished this first by forming the variance/covariance matrix in time, then subjecting that matrix to an Hilbert transform, and finally by performing singular value decomposition (SVD) on the resulting complex expression of the temporal data[8]. The spatial parts of the CEOFs are the products of the matrix of temporal eigenfunctions from the SVD and the original data sequence. We then obtained a revised data sequence by reconstruction from the first two CEOFs, representing 55% of the original data. Fig. 2 shows the real part of this reconstruction. The color scale emphasizes the peaks (red) and troughs (blue) of the fluctuations. A number of patterns appear to propagate most of the way around Antarctica. One of these starts propagating eastward as a peak in 1981 at about 80°E. It appears to move at an unsteady speed. In 1985, it reached 150°W where it strengthened. At this point, weak troughs developed on either side of the peak, becoming deeper during 1984-86 as the unsteady eastward propagation continues. The eastern trough formed west of the Palmer Peninsula in 1984, but in 1985 and onwards was located east of that peninsula. By 1987, the peak had also crossed into the Weddell Sea. A second peak is evident at this time, located at about 150°E, thus forming a peak-trough-peak-trough pattern that propagated eastward. In 1989, the first peak in centered at about 30°E, appearing on each side of the figure. By 1990, the original trough-peak-trough has propagated further eastward, but weakened in intensity. The eastward trough of the second group led the second peak around the Palmer Peninsula into the Weddell Sea as time proceeds until 1992, after which the pattern dissipated. Thus during most of the time sequence illustrated in Fig. 2, eastward propagation of waves of SIC in the interior of the ice pack can be seen to dominate the interannual variability, in concert with the observed propagation of the SST as depicted in Fig. 1. It has the characteristic global wavenumber 2 pattern found in SSTs, but the eastward phase propagation in the sea ice is less steady than in SST and the spatial patterns are not as smooth. We note too that the eastward propagation occurring in these averaged JJASON data might well be more complicated on shorter time intervals.

To illustrate more clearly the relationship between SSTs and the adjacent SICs, we have mapped in Fig. 3 the SSTs together with the corresponding SICs averaged over JJASON for the years 1983-1986. We pick up the ACW in 1983 the first trough-peak-trough SIC signal discussed earlier, in the same location as in Fig. 2. Eastward propagation of the SIC signal is even more evident in this polar projection view. What is remarkable is the like-propagation of a corresponding peak-trough-peak pattern in the

SSTs (the "hot" and "cold" colors have been reversed for the SSTs to enhance the visualization), in concert with the intuitive notion that colder SSTs would give rise to higher SICs. Even more remarkable is the continuation of the contour patterns in the SSTs into the SICs across the boundary between the open ocean and the sea ice. Notice that the peak corresponding to the second one described in Fig. 2 does not appear to be as closely correlated with the adjacent SSTs, although we speculate that the SIC anomaly may be in its formative stage. Correspondingly, we also speculate that where more dense SICs are near higher SSTs (e.g., at 0° longitude in 1985), the SICs may be going through decay. The entire circumpolar SST pattern appears to rotate eastward (cyclonically) while changing its shape noticeably. A complete rotation of the SST is not achieved during this 4-year period; that nominally requires 8 years[1-3] (Fig. 1**c**).

We conclude with the intuitive idea that warmer SSTs are associated with less dense SICs, and visa versa, during JJASON when sea ice extent is near its annual maximum. It is not possible to determine cause and effect on the basis of our present observations. However the annual disappearance and re-emergence of the sea ice field at the beginning and end of every summer indicates that the upper ocean temperatures carry the memory of the ACW into the sea ice field from one winter to the next. Because of the high heat capacity of the ocean, we speculate that the SSTs drive the SICs through either their thermal influence on sea ice formation and/or upon their influence on associated meridional surface winds, the latter observed earlier[1-3] to be poleward (equatorward) over warm (cool) SSTs[9]. This offers the possibility of predicting winter SICs from one year to the next in the same way that the ACW has been used to predict winter temperature and precipitation over New Zealand[10].

1. White, W.B. and Peterson, R. 1996. An Antarctic circumpolar wave in surface pressure, wind, temperature, and sea ice extent. *Nature*, **380**, 699-702.
2. Jacobs, G.A. and Mitchell, J.L., 1996. Ocean circulation variations associated with the Antarctic Circumpolar Wave, *Geophys. Res. Letters*, **23**, 2947-2950.
3. Peterson, R.G. and White, W.B. 1998. Slow oceanic teleconnections linking the Antarctic Circumpolar Wave with tropical ENSO. *J. Geophys. Res.* ,**103**, 24,573-24,583.
4. Reynolds R.W. and Marsico, D.C. 1993. An improved real-time global sea surface temperature analysis. *J. Clim.*, **6**, 114-119.
5. National Snow and Ice Center, 1997. *Nimbus-7 SMMR Arctic and Antarctic sea ice concentration grids, 10/78-8/87; OMSP F8 SSM/I ice concentration grids for Polar regions, 7/87-12/96*, provided on CD-ROM by the National Snow and Ice Data Center, Boulder, Colorado.
6. Kaylor, R.E., 1977. Filtering and decimation of digital time series. *Inst. Phys. Sci, and Tech., U. of Maryland, College Park. Tech Rpt. Note BN 850*, 14 pp.
7. Kalnay and co-authors, 1996. The NCEP/NCAR 40-year reanalysis project. *Bull. Amer. Meteorol. Soc.*, **77**, 437-471.

8. Preisendorfer, R.W. and C.D Mobley, 1988. *Principal Component Analysis in Meteorology and Oceanography*, , 425 pp, Elsevier, Amsterdam, The Netherlands.
9. White, W.B., S.-C. Chen, and R.G. Peterson, 1998. The Antarctic Circumpolar Wave: A beta-effect in ocean-atmosphere coupling over the Southern Ocean. *J. Phys. Oceanogr.*, **28**, 2345-2361.
10. White, W.B. and N. J. Cherry, 1999. Influence of the Antarctic circumpolar wave upon New Zealand temperature and precipitation during autumn-winter. *J. Clim.*, **12**, 960-976.

Acknowledgements

We thank A.E Walker for organizing and analyzing the data sets. The NASA Office of Polar Programs and the NOAA Office of Global Programs supported this work.

Figure Captions

Fig. 1. Time/longitude plots of **a**. residual extents of sea ice (0.5° longitude intervals), **b**. residuals of average sea ice concentrations in 1° sectors (5% intervals), and **c**. residual sea surface temperatures (0.25°C intervals). All shaded contours are negative values. Residuals were obtained by subtracting the shared 18-year average of JJASONs, then a band-pass filter further smoothed each parameter (see text). **d.** Time-lag correlations are shown for the extent of sea ice (ESI) vs. average sea ice concentration (ASIC), SIE vs. sea surface temperature (SST), and SIC vs. SST.

Fig. 2. A 16-year sequence of reconstructed residual sea ice concentrations (SICs)[5] averaged for JJASON for each year from 1980-1995, depicting the eastward progression of spatial waves in the SICs. These residuals were reconstructed from the first two complex empirical orthogonal functions obtained from band-pass filtering (see text) differences between each 6-month average and their 16-year average.

Fig. 3. Four of the 16 years of SIC data shown in Fig. 2 are replotted here in a polar stereographic projection, along with similarly averaged and filtered sea surface temperatures (SSTs)[4]. Here the negative SST residuals are shown as "warm" colors to enhance the remarkable connection between colder (warmer) SST patterns and more (less) dense SIC patterns as they progress eastward from about 90°E to 45°W. The white band separating the two data fields arises from the southernmost limit of the SST data and the northernmost limit of the SICs, as here averaged.

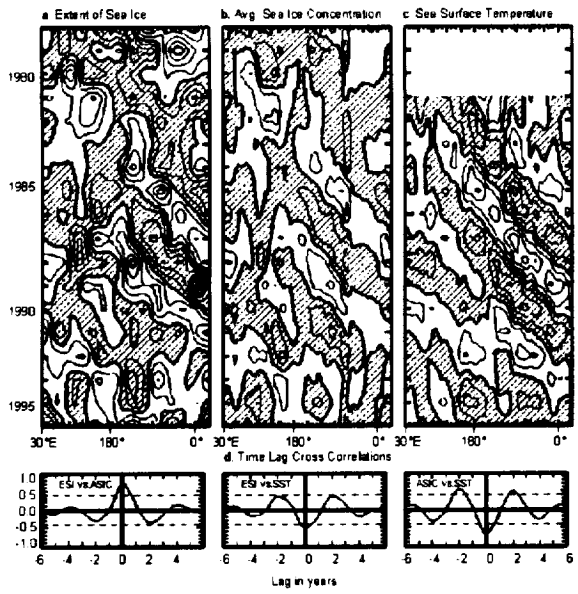

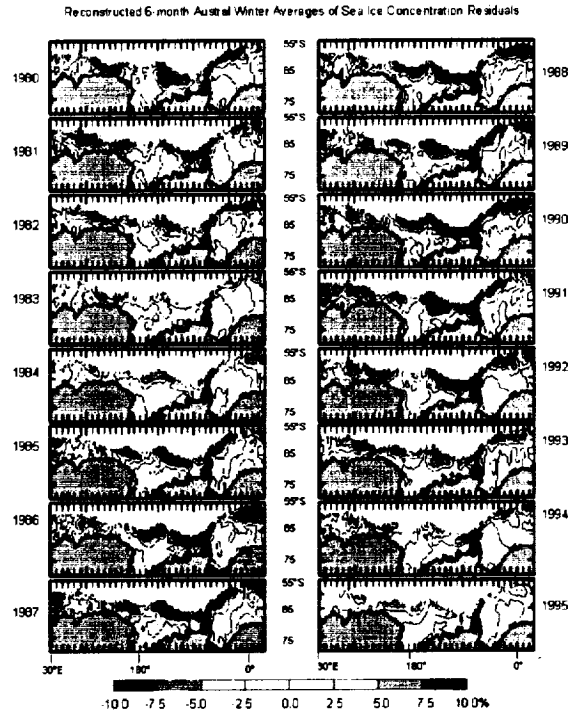

Sea Surface Temperature and Sea Ice Concentration Residuals